JOURNAL OF COMPUTATIONAL PHYSICS 74, 25–40 (1988)

Numerical Solution of Eigenvalue Problems Using the Compound Matrix Method

STERGIOS G. YIANTSIOS AND BRIAN G. HIGGINS

Department of Chemical Engineering, University of California, Davis, California 95616

Received July 25, 1986; revised February 6, 1987

An algorithm based on the compound matrix method is presented for solving difficult eigenvalue problems. Details are given for systems of ordinary differential equations of fourth-order that are valid over connected domains coupled through interfacial conditions. As an example we examine the linear stability of two superposed fluids in plane Poiseuille flow and consider both interfacial and shear modes. The Orr–Sommerfeld system that describes linear stability is solved for a selected range of parameters. © 1988 Academic Press, Inc.

1. INTRODUCTION

In a series of papers Ng and Reid [4–6] and Davey [1] discuss the application of the compound matrix method for the numerical solution of linear two-point boundary value and eigenvalue problems involving stiff differential operators with separated boundary conditions. The basic idea of the compound matrix method is to convert a stiff two-point boundary value problem into an initial value problem that can be solved by standard shooting techniques. This is done by first computing the appropriate compound of the solution matrix (subject to prescribed initial conditions) by numerically integrating as an initial value problem the compound differential equation set the compound satisfies. In the case of an eigenvalue problem the integration of the compound differential system is also subject to satisfying an eigenvalue relation that is derived from the boundary conditions of the original problem. Once the compound has been determined numerically, an auxiliary set of equations (of lower order than the original problem) is then integrated backwards to determine the eigenfunction. The coefficients of the auxiliary set of equations are known in terms of the components of the compound.

In this paper we demonstrate that the compound matrix method can be applied to equation sets valid over connected domains coupled through interfacial conditions. In particular we examine an eigenvalue problem that describes the linear stability of superposed Newtonian fluids in plane Poiseuille flow. Such a flow may be unstable to an interfacial mode as well as a shear mode. In the case of the shear mode, the differential operator is known to be stiff, in the sense that its solutions have widely differing growth rates.

0021-9991/88 $3.00

In Section 2 we present a general algorithm for the compound matrix method for an eigenvalue problem described by two fourth-order linear systems valid over connected domains. The algorithm is based on the work of Ng and Reid [6] and Schwarz [7]. We derive the necessary eigenvalue relation and show how it may be expressed in terms of the compounds of the solution matrices for each fourth-order system.

In Section 3 we present the details of the algorithm for solving the linear stability of two superposed fluids in plane Poiseuille flow. We also discuss how the algorithm relates to the stability of a single fluid. In Section 4 sample calculations for an interfacial mode and shear mode are given and the neutral stability curve for the shear mode is presented for a specific case.

2. Compound Matrix Method Algorithm

To illustrate the method for eigenvalue problems with interfacial conditions we will consider the following linear homogeneous system

$$\boldsymbol{\phi}' = \mathbf{F}\boldsymbol{\phi}, \qquad 0 \leqslant x \leqslant 1, \tag{1a}$$

$$\boldsymbol{\psi}' = \mathbf{G}\boldsymbol{\psi}, \qquad -n \leqslant x \leqslant 0, \tag{1b}$$

where $\mathbf{F}(x) = [f_{ij}(x)]$, $\mathbf{G}(x) = [g_{ij}(x)]$ are 4×4 matrices and the solutions $\boldsymbol{\phi} = [\phi_j(x)]$, $\boldsymbol{\psi} = [\psi_j(x)]$ are 4×1 column vectors. We suppose that the boundary conditions at $x = 1$ and $x = -n$ are separated and are given by

$$\mathbf{R}\boldsymbol{\phi}(1) = 0, \tag{2a}$$

and

$$\mathbf{Q}\boldsymbol{\psi}(-n) = 0, \tag{2b}$$

where $\mathbf{R}$ and $\mathbf{Q}$ are 2×4 matrices. At the interface located at $x = 0$ we have

$$\mathbf{P}\boldsymbol{\phi}(0) + \mathbf{S}\boldsymbol{\psi}(0) = 0, \tag{3}$$

where $\mathbf{P}$ and $\mathbf{S}$ are 4×4 matrices.

Let $\boldsymbol{\phi}_1$, $\boldsymbol{\phi}_2$ be any two linearly independent solutions of (1a) that satisfy the initial conditions (2a). The second compound $\mathbf{y}$ of the 4×2 solution matrix $\boldsymbol{\Phi} = [\boldsymbol{\phi}_1, \boldsymbol{\phi}_2]$ is a 6×1 matrix having minors of $\boldsymbol{\Phi}$ as elements:

$$y(i, j) = \phi_{1i}\phi_{2j} - \phi_{1j}\phi_{2i}, \tag{4a}$$

where $i = 1, 2, 3$ and $j = i + 1, ..., 4$. In lexicographic order of their indices the elements of $\mathbf{y}$ are

$$y_1 = y(1, 2), \qquad y_2 = y(1, 3), \qquad \cdots, \qquad y_6 = y(3, 4). \tag{4b}$$

Using the algorithm provided by Schwartz [7], one can show that the differential compound system for $\mathbf{y}=[y_1, y_2, ..., y_6]^{\mathrm{T}}$ is given by

$$\mathbf{y}'=\mathbf{H}(x)\,\mathbf{y}, \tag{5}$$

where the elements of $\mathbf{H}(x)$ are known in terms of the elements of $\mathbf{F}$:

$$\mathbf{H}=\begin{bmatrix} f_{11}+f_{22} & f_{23} & f_{24} & -f_{13} & -f_{14} & 0 \\ f_{32} & f_{11}+f_{33} & f_{34} & f_{12} & 0 & -f_{14} \\ f_{42} & f_{43} & f_{11}+f_{44} & 0 & f_{12} & f_{13} \\ -f_{31} & f_{21} & 0 & f_{22}+f_{33} & f_{34} & -f_{24} \\ -f_{41} & 0 & f_{21} & f_{43} & f_{22}+f_{44} & f_{23} \\ 0 & -f_{41} & f_{31} & -f_{42} & f_{32} & f_{33}+f_{44} \end{bmatrix}. \tag{6}$$

The initial condition that $\mathbf{y}$ satisfies can be found from (4a) using (2a). Similarly, if $\mathbf{z}=[z_1, ..., z_6]^{\mathrm{T}}$ is the second compound of the solution matrix $\mathbf{\Psi}=[\boldsymbol{\psi}_1, \boldsymbol{\psi}_2]$, the differential compound system for $\mathbf{z}$ is

$$\mathbf{z}'=\mathbf{I}(x)\,\mathbf{z}, \tag{7}$$

where as before the elements of $\mathbf{I}$ are known in terms of the elements of $\mathbf{G}$ in the manner indicated by (6). $\boldsymbol{\psi}_1, \boldsymbol{\psi}_2$ are linearly independent solutions of (1b) that satisfy the initial conditions (2b).

In general, the solutions of (1a), (1b) consistent with boundary conditions at $x=1$ and $x=-n$ will have the form

$$\boldsymbol{\phi}=\kappa\boldsymbol{\phi}_1+\lambda\boldsymbol{\phi}_2, \tag{8a}$$

$$\boldsymbol{\psi}=\mu\boldsymbol{\psi}_1+\sigma\boldsymbol{\psi}_2. \tag{8b}$$

We can express the interfacial condition (3) in terms of $\boldsymbol{\phi}_1(0)$, $\boldsymbol{\phi}_2(0)$, $\boldsymbol{\psi}_1(0)$, $\boldsymbol{\psi}_2(0)$, and a vector of constants $\mathbf{u}=[\kappa, \lambda, \mu, \sigma]^{\mathrm{T}}$ as follows

$$\mathbf{Cu}=0, \tag{9}$$

where

$$\mathbf{C}=\begin{bmatrix} \mathbf{p}_1^T\boldsymbol{\phi}_1 & \mathbf{p}_1^T\boldsymbol{\phi}_2 & \mathbf{s}_1^T\boldsymbol{\psi}_1 & \mathbf{s}_1^T\boldsymbol{\psi}_2 \\ \mathbf{p}_2^T\boldsymbol{\phi}_1 & \mathbf{p}_2^T\boldsymbol{\phi}_2 & \mathbf{s}_2^T\boldsymbol{\psi}_1 & \mathbf{s}_2^T\boldsymbol{\psi}_2 \\ \mathbf{p}_3^T\boldsymbol{\phi}_1 & \mathbf{p}_3^T\boldsymbol{\phi}_2 & \mathbf{s}_3^T\boldsymbol{\psi}_1 & \mathbf{s}_3^T\boldsymbol{\psi}_2 \\ \mathbf{p}_4^T\boldsymbol{\phi}_1 & \mathbf{p}_4^T\boldsymbol{\phi}_2 & \mathbf{s}_4^T\boldsymbol{\psi}_1 & \mathbf{s}_4^T\boldsymbol{\psi}_2 \end{bmatrix}. \tag{10}$$

Note, in deriving (10) we have partitioned $\mathbf{P}$ and $\mathbf{S}$ as follows

$$\mathbf{P}=\begin{bmatrix} \mathbf{p}_1^T \\ \mathbf{p}_2^T \\ \mathbf{p}_3^T \\ \mathbf{p}_4^T \end{bmatrix}, \qquad \mathbf{S}=\begin{bmatrix} \mathbf{s}_1^T \\ \mathbf{s}_2^T \\ \mathbf{s}_3^T \\ \mathbf{s}_4^T \end{bmatrix}.$$

For a nontrivial solution we require

$$\det(\mathbf{C}) = 0, \tag{11}$$

On using Laplace's expansion of a determinant by complementary minors, we obtain

$$\begin{aligned}\det(\mathbf{C}) = {} & [(\mathbf{s}_1^{\mathrm{T}}\boldsymbol{\psi}_1)(\mathbf{s}_2^{\mathrm{T}}\boldsymbol{\psi}_2) - (\mathbf{s}_1^{\mathrm{T}}\boldsymbol{\psi}_2)(\mathbf{s}_2^{\mathrm{T}}\boldsymbol{\psi}_1)][(\mathbf{p}_3^{\mathrm{T}}\boldsymbol{\phi}_1)(\mathbf{p}_4^{\mathrm{T}}\boldsymbol{\phi}_2) - (\mathbf{p}_3^{\mathrm{T}}\boldsymbol{\phi}_2)(\mathbf{p}_4^{\mathrm{T}}\boldsymbol{\phi}_1)] \\ & - [(\mathbf{s}_3^{\mathrm{T}}\boldsymbol{\psi}_2)(\mathbf{s}_1^{\mathrm{T}}\boldsymbol{\psi}_1) - (\mathbf{s}_1^{\mathrm{T}}\boldsymbol{\psi}_2)(\mathbf{s}_3^{\mathrm{T}}\boldsymbol{\psi}_1)][(\mathbf{p}_2^{\mathrm{T}}\boldsymbol{\phi}_1)(\mathbf{p}_4^{\mathrm{T}}\boldsymbol{\phi}_2) - (\mathbf{p}_4^{\mathrm{T}}\boldsymbol{\phi}_1)(\mathbf{p}_1^{\mathrm{T}}\boldsymbol{\phi}_2)] \\ & - [(\mathbf{s}_1^{\mathrm{T}}\boldsymbol{\psi}_2)(\mathbf{s}_4^{\mathrm{T}}\boldsymbol{\psi}_1) - (\mathbf{s}_4^{\mathrm{T}}\boldsymbol{\psi}_2)(\mathbf{s}_1^{\mathrm{T}}\boldsymbol{\psi}_1)][(\mathbf{p}_2^{\mathrm{T}}\boldsymbol{\phi}_1)(\mathbf{p}_3^{\mathrm{T}}\boldsymbol{\phi}_2) - (\mathbf{p}_3^{\mathrm{T}}\boldsymbol{\phi}_1)(\mathbf{p}_2^{\mathrm{T}}\boldsymbol{\phi}_2)] \\ & - [(\mathbf{s}_2^{\mathrm{T}}\boldsymbol{\psi}_2)(\mathbf{s}_3^{\mathrm{T}}\boldsymbol{\psi}_1) - (\mathbf{s}_3^{\mathrm{T}}\boldsymbol{\psi}_2)(\mathbf{s}_1^{\mathrm{T}}\boldsymbol{\psi}_1)][(\mathbf{p}_1^{\mathrm{T}}\boldsymbol{\phi}_1)(\mathbf{p}_4^{\mathrm{T}}\boldsymbol{\phi}_2) - (\mathbf{p}_4^{\mathrm{T}}\boldsymbol{\phi}_1)(\mathbf{p}_1^{\mathrm{T}}\boldsymbol{\phi}_2)] \\ & - [(\mathbf{s}_4^{\mathrm{T}}\boldsymbol{\psi}_2)(\mathbf{s}_2^{\mathrm{T}}\boldsymbol{\psi}_1) - (\mathbf{s}_2^{\mathrm{T}}\boldsymbol{\psi}_2)(\mathbf{s}_4^{\mathrm{T}}\boldsymbol{\psi}_1)][(\mathbf{p}_1^{\mathrm{T}}\boldsymbol{\phi}_1)(\mathbf{p}_3^{\mathrm{T}}\boldsymbol{\phi}_2) - (\mathbf{p}_3^{\mathrm{T}}\boldsymbol{\phi}_1)(\mathbf{p}_1^{\mathrm{T}}\boldsymbol{\phi}_2)] \\ & - [(\mathbf{s}_3^{\mathrm{T}}\boldsymbol{\psi}_2)(\mathbf{s}_4^{\mathrm{T}}\boldsymbol{\psi}_1) - (\mathbf{s}_4^{\mathrm{T}}\boldsymbol{\psi}_2)(\mathbf{s}_3^{\mathrm{T}}\boldsymbol{\psi}_1)][(\mathbf{p}_1^{\mathrm{T}}\boldsymbol{\phi}_1)(\mathbf{p}_2^{\mathrm{T}}\boldsymbol{\phi}_2) - (\mathbf{p}_1^{\mathrm{T}}\boldsymbol{\phi}_2)(\mathbf{p}_2^{\mathrm{T}}\boldsymbol{\phi}_1)].\end{aligned} \tag{12}$$

The appropriate eigenvalue relation is derived by expressing $\det(\mathbf{C})$ in terms of the compounds $\mathbf{y}$ and $\mathbf{z}$. The terms in the brackets are similar in form and thus it is sufficient to show that any one of the 12 terms can be expressed in terms of the compounds. Let $\boldsymbol{\phi}_i = [\phi_{i1}, ..., \phi_{i4}]^{\mathrm{T}}$ and $\mathbf{p}_i = [p_{i1}, ..., p_{i4}]^{\mathrm{T}}$, then after some manipulation one can show that

$$\begin{aligned}(\mathbf{p}_i^{\mathrm{T}}\boldsymbol{\phi}_1)(\mathbf{p}_j^{\mathrm{T}}\boldsymbol{\phi}_2) - (\mathbf{p}_j^{\mathrm{T}}\boldsymbol{\phi}_1)(\mathbf{p}_i^{\mathrm{T}}\boldsymbol{\phi}_2) = {} & (p_{i1}p_{j2} - p_{i2}p_{j1})\,y_1 + (p_{i1}p_{j3} - p_{i3}p_{j1})\,y_2 \\ & + (p_{i1}p_{j4} - p_{i4}p_{j1})\,y_3 + (p_{i2}p_{j3} - p_{i3}p_{j2})\,y_4 \\ & + (p_{i2}p_{j4} - p_{i4}p_{j2})\,y_5 + (p_{i3}p_{j4} - p_{i4}p_{j3})\,y_6,\end{aligned} \tag{13}$$

where $y_1, ..., y_6$ are the components of the second compound of $\boldsymbol{\Phi}$ and $i \neq j$. Similar expressions can be derived for the remaining 11 terms in (12).

The key to the success of the compound matrix method is that the eigenvalue relation can be expressed in terms of the compounds $\mathbf{y}(0)$ and $\mathbf{z}(0)$, which in turn can be determined by integrating (5) and (7) from the boundary points 1 and $-n$ toward the interface at $x = 0$. At $x = 0$ the eigenvalue relation $\det(\mathbf{C}) = 0$ must be satisfied and this is achieved by varying the eigenvalue parameter using a suitable iterative procedure.

After the determination of the eigenvalue, one can proceed to determine the eigenfunctions $\boldsymbol{\phi}$ and $\boldsymbol{\psi}$ from a set of auxiliary equations that may be derived from the elimination of $\kappa, \lambda, \mu, \sigma$ from (8). For a fixed i, j with $i \neq j$ one can easily show (Ng and Reid [6]) that

$$\phi'_i\, y(i,j) = f_{ik}[\,y(k,j)\,\phi_i - y(k,i)\,\phi_j] \tag{14a}$$

$$\phi'_j\, y(i,j) = f_{jk}[\,y(k,j)\,\phi_i - y(k,i)\,\phi_j], \tag{14b}$$

where the summation is over the index k. The compound elements $y(i,j)$ are defined in (4a). A similar set of auxiliary equations may be derived for ψ_i, ψ_j. Any two equations from (14) can be used to determine ϕ_i, ϕ_j though some sets may be more appropriate (Ng and Reid [4]). The auxiliary equations for $\boldsymbol{\phi}$ and $\boldsymbol{\psi}$ are integrated backwards to boundary points 1 and $-n$ once the initial conditions for the backward integration are found. Because of the unwieldy algebra, the details of this step for the general case are not given. In the example problem discussed below, the procedure for finding $\boldsymbol{\phi}(0)$, $\boldsymbol{\psi}(0)$ is outlined.

3. Example: Linear Stability of Superposed Fluids

We consider plane Poiseuille flow of two superposed liquids of different viscosity. The dimensionless velocity profiles for the base flow are

$$U_1 = 1 + a_1 x + b_1 x^2, \qquad 0 \leqslant x \leqslant 1,$$

and (15)

$$U_2 = 1 + a_2 x + b_2 x^2, \qquad -n \leqslant x \leqslant 0,$$

where

$$a_1 = \frac{m - n^2}{n^2 + n}, \qquad b_1 = -\frac{m+n}{n+n^2}, \qquad a_2 = \frac{a_1}{m}, \qquad b_2 = \frac{b_1}{m}. \tag{16}$$

The subscripts 1, 2 denote the upper and lower fluid, respectively; m and n are the viscosity and thickness ratios defined in terms of the lower fluid with respect to the upper. Linear stability analysis of the base flow (15) leads to the familiar Orr–Sommerfeld equation for the amplitude of the disturbance stream function for each fluid layer (Yih [11]). Let $\boldsymbol{\phi}$ be the solution vector that satisfies the Orr–Sommerfeld equation for the upper layer (expressed as a system of first-order equations as in (1)). Then the nonzero elements of $\mathbf{F}$ are

$$\begin{gathered} f_{12} = f_{23} = f_{34} = 1, \\ f_{41} = -\{\alpha^4 + i\alpha R[\alpha^2(U_1 - c) + U_1'']\}, \qquad f_{43} = 2\alpha^2 + i\alpha R(U_1 - c). \end{gathered} \tag{17}$$

Similarly if $\boldsymbol{\psi}$ is the solution vector that satisfies the Orr–Sommerfeld equations for the lower layer, the nonzero elements of $\mathbf{G}$ are

$$\begin{gathered} g_{12} = g_{23} = g_{34} = 1, \\ g_{41} = -\left\{\alpha^4 + i\alpha \frac{Rr}{m}[\alpha^2(U_2 - c) + U_2'']\right\}, \qquad g_{43} = 2\alpha^2 + i\alpha \frac{Rr}{m}(U_2 - c) \end{gathered} \tag{18}$$

where $r = \rho_2/\rho_1$ is the density ratio, $R = \rho_1 U_0 d_1/\mu_1$ the Reynolds number (U_0 being the interfacial velocity, and d_1 the thickness of the upper layer), α the wavenumber of the disturbance, and c the complex wave speed of the disturbance.

The no-slip and impenetrability conditions on $\boldsymbol{\phi}$ and $\boldsymbol{\psi}$ at the channel walls $x=1$, $x=-n$ determine the nonzero elements of $\mathbf{R}$ and $\mathbf{Q}$ in (2):

$$r_{11}=r_{21}=1, \qquad q_{11}=q_{21}=1. \tag{19}$$

Continuity of velocity and stresses at the interface $x=0$ yield the nonzero elements of $\mathbf{P}$ and $\mathbf{S}$:

$$\begin{aligned} &p_{11}=1, \qquad p_{21}=-\frac{(a_2-a_1)}{c-1}, \qquad p_{22}=1,\\ p_{31}=\alpha^2, \qquad &p_{33}=1, \qquad p_{41}=-i\alpha R[a_1+(F+\alpha^2 S)/(c-1)],\\ &p_{42}=3\alpha^2-i\alpha R(c-1), \qquad p_{44}=-1, \end{aligned} \tag{20a}$$

and

$$\begin{aligned} &s_{11}=-1, \qquad s_{22}=-1, \qquad s_{31}=-m\alpha^2, \qquad s_{33}=-m,\\ &s_{41}=i\alpha Rra_2, \qquad s_{42}=-3m\alpha^2+i\alpha Rr(c-1), \qquad s_{44}=m. \end{aligned} \tag{20b}$$

Here $F=(r-1)\,gd_1/U_0^2$ and $S=\sigma/\rho_1 d_1 U_0^2$ are the dimensionless groups expressing the effects of gravity g and interfacial tension σ. For a discussion on the derivation of the interfacial conditions (20), the reader is referred to the paper by Yih [11].

Now let $\boldsymbol{\phi}_1$ and $\boldsymbol{\phi}_2$ be two solutions of (1a) that satisfy the initial conditions (2a) (see also (19))

$$\boldsymbol{\phi}_1(1)=[0,0,1,0]^{\mathrm{T}}, \qquad \boldsymbol{\phi}_2(1)=[0,0,0,1]^{\mathrm{T}}, \tag{21}$$

and similarly let $\boldsymbol{\psi}_1$, $\boldsymbol{\psi}_2$ be two solutions of (16) that satisfy the initial conditions (2b) (see also (19))

$$\boldsymbol{\psi}_1(-n)=[0,0,1,0]^{\mathrm{T}}, \qquad \boldsymbol{\psi}_2(-n)=[0,0,0,1]^{\mathrm{T}}. \tag{22}$$

Then from (5) we find that the second compound $\mathbf{y}$ of $\boldsymbol{\Phi}$ satisfies

$$\begin{aligned} &y_1'=y_2, \qquad y_2'=y_3+y_4,\\ &y_3'=f_{43}\,y_2+y_5, \qquad y_4'=y_5,\\ &y_5'=-f_{41}\,y_1+f_{43}\,y_4+y_6, \qquad y_6'=-f_{41}\,y_2. \end{aligned} \tag{23}$$

The initial condition for $\mathbf{y}$ follows from (21) and (4a):

$$\mathbf{y}(1)=[0,0,0,0,0,1]^{\mathrm{T}}. \tag{24}$$

Similarly the second compound $\mathbf{z}$ of $\boldsymbol{\Psi}$ satisfies the same set of equations with f_{43} and f_{41} replaced with g_{43} and g_{41}. The same initial condition for $\mathbf{z}$ as in (24) applies also at $x=-n$.

At $x=0$, we assume that the vectors $\boldsymbol{\phi}_1, \boldsymbol{\phi}_2, \boldsymbol{\psi}_1, \boldsymbol{\psi}_2$ take the values

$$\begin{aligned} \boldsymbol{\phi}_1(0) &= [\phi_{11}, \phi_{12}, \phi_{13}, \phi_{14}]^{\mathrm{T}}, \qquad & \boldsymbol{\phi}_2(0) &= [\phi_{21}, \phi_{22}, \phi_{23}, \phi_{24}]^{\mathrm{T}} \\ \boldsymbol{\psi}_1(0) &= [\psi_{11}, \psi_{12}, \psi_{13}, \psi_{14}]^{\mathrm{T}}, \qquad & \boldsymbol{\psi}_2(0) &= [\psi_{21}, \psi_{22}, \psi_{23}, \psi_{24}]^{\mathrm{T}}. \end{aligned} \tag{25}$$

Thus the matrix $\mathbf{C}$ is given by

$$C = \begin{bmatrix} \phi_{11} & \phi_{21} & -\psi_{11} & -\psi_{21} \\ \phi_{12} + \dfrac{a_1 - a_2}{c_1}\phi_{11} & \phi_{22} + \dfrac{a_1 - a_2}{c_1}\phi_{21} & -\psi_{12} & -\psi_{22} \\ \phi_{13} + \alpha^2\phi_{11} & \phi_{23} + \alpha^2\phi_{21} & -m(\psi_{13} + \alpha^2\psi_{11}) & -m(\psi_{23} + \alpha^2\psi_{21}) \\ \begin{gathered} -i\alpha R(c_1\phi_{12} + a_1\phi_{11}) \\ -\phi_{14} + 3\alpha^2\phi_{12} \\ -i\alpha R(F + \alpha^2 S)\dfrac{\phi_{11}}{c_1} \end{gathered} & \begin{gathered} -i\alpha R(c_1\phi_{22} + a_1\phi_{21}) \\ -\phi_{24} + 3\alpha^2\phi_{22} \\ -i\alpha R(F + \alpha^2 S)\dfrac{\phi_{21}}{c_1} \end{gathered} & \begin{gathered} i\alpha Rr(c_1\psi_{12} + a_2\psi_{11}) \\ +m(\phi_{14} - 3\alpha^2\psi_{12}) \\ \end{gathered} & \begin{gathered} i\alpha Rr(c_1\psi_{22} + a_2\psi_{21}) \\ +m(\psi_{24} - 3\alpha^2\psi_{22}) \\ \end{gathered} \end{bmatrix}. \tag{26}$$

The existence of nontrivial solutions requires that $\det(\mathbf{C}) = 0$ and expanding the determinant we derive the appropriate eigenvalue relation in terms of the compounds $\mathbf{y}$ and $\mathbf{z}$:

$$\begin{aligned} &[z_1 y_1 \alpha^2(m-1) + z_1 y_4 - m z_4 y_1][3\alpha^2(m-1) - i\alpha R c_1(r-1)] \\ &\quad + z_1 y_2\left[-i\alpha R(r-1)\, a_1 + 3\alpha^2 m\frac{(a_1 - a_2)}{c_1} + i\alpha R\frac{(F + \alpha^2 S)}{c_1}\right] \\ &\quad + (z_1 y_3 - m z_3 y_1)\,\alpha^2(m-1) + (z_2 y_3 - z_3 y_2)\, m\frac{(a_1 - a_2)}{c_1} \\ &\quad - (z_1 y_6 + m^2 z_6 y_1) + m(z_2 y_5 + z_5 y_2) - m(z_3 y_4 + z_4 y_3) \\ &\quad + z_2 y_1 m\left[i\alpha R(r-1)\, a_2 - 3\alpha^2\frac{(a_1 - a_2)}{c_1} - i\alpha R\frac{(F + \alpha^2 S)}{c_1}\right] = 0. \end{aligned} \tag{27}$$

For convenience we have defined $c_1 \equiv c - 1$.

For the backward integration we set $i = 1, j = 2$ in (14). The auxiliary equations for $\boldsymbol{\phi}$ and $\boldsymbol{\psi}$ are then

$$y_1\phi_2' - y_2\phi_2 + y_4\phi_1 = 0, \qquad \phi_1' = \phi_2, \tag{28}$$

and

$$z_1\psi_2' - z_2\psi_2 + z_4\psi_1 = 0, \qquad \psi_1' = \psi_2. \tag{29}$$

One can normalize $\phi_1(0)=\psi_1(0)=1$, and the initial conditions on $\phi_2(0)$ and $\psi_2(0)$ can be found as follows. Equations (28) and (29) are evaluated at $x=0$. At the interface it follows from (20) and (3) that

$$\phi_2(0)-\psi_2(0)-\phi_1(0)\frac{(a_2-a_1)}{c_1}=0, \tag{30}$$

$$\phi_3(0)+\alpha^2\phi_1(0)-m[\psi_3(0)+\alpha^2\psi_1(0)]=0, \tag{31}$$

and from (17) and (18) we have

$$\phi_2'=\phi_3, \qquad \psi_2'=\psi_3. \tag{32}$$

Thus ϕ_2' and ψ_2' may be eliminated from (28) and (29) with the use of (30), (31), and (32). The result is

$$(z_1 y_2-my_1z_2)\,\phi_2(0)=\left[z_1 y_1\alpha^2(m-1)+z_1 y_4-mz_4 y_1+\frac{(a_1-a_2)}{c_1}my_1z_1\right]\phi_1(0). \tag{33}$$

Once $\phi_2(0)$ is determined, (30) can be used to find $\psi_2(0)$.

It is interesting to see how the above procedure relates back to the problem of stability of a single fluid elaborated on by Ng and Reid [4]. In this case $m=r=n=1$, $F=S=0$, $a_1=a_2=0$, and $b_1=b_2=1$. The channel walls are now at $x=\pm 1$, and from (17) and (18) it follows that

$$f_{43}(1-x)=g_{43}(x-1), \qquad f_{41}(1-x)=g_{41}(x-1). \tag{34a}$$

The same relationships hold for the second derivatives of the above, viz.,

$$f_{43}''(1-x)=g_{43}''(x-1), \qquad f_{41}''(1-x)=g_{41}''(x-1), \tag{34b}$$

while the first derivatives are of opposite sign, viz.,

$$f_{43}'(1-x)=-g_{43}'(x-1), \qquad f_{41}'(1-x)=-g_{41}'(x-1). \tag{34c}$$

Using (23) and the initial condition (24), we can write a Taylor series for **y** around the point $x=1$, and the same can be done for **z** around $x=-1$. For example, consider the Taylor series for y_1 and z_1:

$$\begin{aligned} y_1(x)&=\frac{2}{4!}(1-x)^4+\frac{3}{6!}f_{43}(1-x)^6+\frac{3}{7!}f_{43}'(1-x)^7\\ &\quad+\frac{(14f_{43}''+3f_{43}^2+4f_{41})}{8!}(1-x)^8+\cdots\\ z_1(-x)&=\frac{2}{4!}(x-1)^4+\frac{3}{6!}g_{43}(x-1)^6+\frac{3}{7!}g_{43}'(x-1)^7\\ &\quad+\frac{(14g_{43}''+3g_{43}^2+4g_{41})}{8!}(x-1)^8+\cdots. \end{aligned} \tag{35}$$

Using the results in (34) it follows then that the coefficients multiplying even and odd powers of $(1-x)$ are even and odd, respectively, which suggests that $y_1(x)=z_1(-x)$. If the radius of convergence of the Taylor series is less than unity, analytic continuation can be invoked to complete the argument. The same is true for y_3, y_4, y_6 and z_3, z_4, z_6 while the opposite holds for y_2, y_5 and z_2, z_5, viz., $y_2(x)=-z_2(-x)$.

Now returning to the interfacial condition (27) and using the above results, we see it reduces to

$$y_1 y_6 + y_2 y_5 + y_3 y_4 = 0. \tag{36}$$

Next we use the quadratic identity (Ng and Reid [4])

$$y_1 y_6 - y_2 y_5 + y_3 y_4 = 0 \tag{37}$$

to show that the interfacial condition for the single fluid case becomes

$$y_2 y_5 = 0. \tag{38}$$

From (4) we see that the vanishing of y_5 corresponds to an even mode for which we require $\phi_2(0)=0$ and (33) agrees with that. The vanishing of y_2 corresponds to an odd mode for which we require $\phi_1(0)=0$. The interfacial condition (33) seems indeterminate. Note, however, that (33) (with $m=1$, $a_1=a_2=0$) may be also expressed as

$$\frac{\phi_1(0)}{\phi_2(0)} = \frac{z_3 y_1 - y_3 z_1}{z_1 y_5 - z_5 y_1}, \tag{39}$$

from which it follows that $\phi_1(0)=0$. To show that (39) is equivalent to (33) (with $m=1$, $a_1=a_2=0$) we must prove that

$$(z_1 y_4 - z_4 y_1)(z_3 y_1 - z_1 y_5) = (z_1 y_2 - y_1 z_2)(z_1 y_5 - z_5 y_1). \tag{40}$$

This is easily done by using the quadratic identity (37) for $\mathbf{y}$ and a similar expression for $\mathbf{z}$ to obtain from (40) the equivalent relation

$$(y_1 z_6 + z_1 y_6) - (z_2 y_5 + y_2 z_5) + (z_3 y_4 + z_4 y_3) = 0. \tag{41}$$

Replacing

$$y_6 = \frac{y_2 y_5 - y_3 y_4}{y_1}, \qquad z_6 = \frac{z_2 z_5 - z_3 z_4}{z_1},$$

we find that the LHS of (41) vanishes identically.

4. Sample Calculations

Yih [11] showed that plane Poiseuille flow of two superposed fluids of different viscosity will be unstable to a small wave number interfacial mode for arbitrary small value of the Reynolds number. The instability is related to the jump in viscosity across the interface. On the other hand, if the Reynolds number is sufficiently high, the flow may also be unstable to a shear mode, which, as is well known, is the unstable mode for the single fluid case (Drazin and Reid [2]). To the best of the authors' knowledge, linear stability of plane Poiseuille flow of two superposed fluids with respect to a shear mode has never been addressed theoretically or numerically in the literature, even though the experiments of Kao and Park [3] suggest that the flow may be unstable to a shear mode.

To illustrate the efficiency of the compound matrix method for studying linear stability of superposed fluids we have performed calculations for large wave numbers and Reynolds numbers where traditional methods such as the standard shooting method and the finite element method (Yiantsios and Higgins [10]) are likely to encounter numerical difficulties. The calculations were done on a VAX 11/785, using a constant step-size fourth-order Runge–Kutta procedure with double precision arithmetic. For almost all cases a step size of 0.001 was adequate to give at least 8-digit accuracy.

For our first sample calculation we examine flow stability with respect to the interfacial mode for large values of the wavenumber α. We have shown previously (Yiantsios and Higgins [9]) by asymptotic methods that in the limit $\alpha \to \infty$ the wave speed $c(=c_r + c_i)$ is given by

$$c = 1 + iR\frac{a_1^2(m-1)^2}{m^2(m+1)}\alpha^{-3}. \tag{42}$$

This formula was derived under the assumptions that $R = O(1)$, $r = 1$, $S = 0$. In Fig. 1 we compare the imaginary part of the wave speed, c_i, calculated by the com-

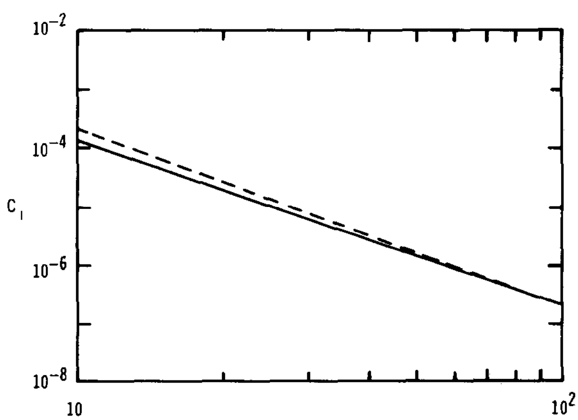

Fig. 1. Imaginary part of the wave speed, c_i, for an unstable interfacial mode versus wavenumber α; --- theoretical value given by Eq. (42). Flow parameters: $m = 5$, $R = 1$, $S = 0$, $r = 1$, $F = 0$, $n = 1$.

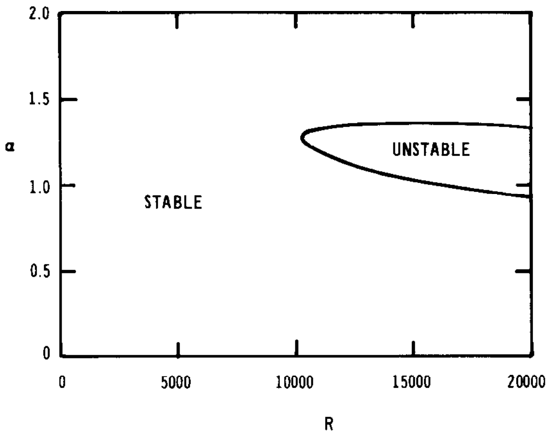

FIG. 2. Neutral stability curve for the shear mode. At criticality $R_c = 10228.8$, $\alpha = 1.274$. Flow parameters: $m = 10$, $r = 1$, $F = 0$, $S = 0$, $n = 1$.

pound matrix method with the value obtained from the above asymptotic formula. For $\alpha > 100$, the numerical value for c_i is indistinguishable from the theoretical value. The values for the flow parameters are indicated in the figure caption. We are also able to reproduce Yih's [11] small wave number results with similar accuracy, though this is not a stringent test of the algorithm since the problem is not numerically stiff at low Reynolds numbers.

Our next sample calculation considers flow stability with respect to a shear mode. In Fig. 2 we plot the neutral stability curve for the shear mode in the plane of the Reynolds number and wave number for a viscosity ratio $m = 10$. In the calculations we have set $n = r = 1$, $F = S = 0$. The critical Reynolds number R_c for the shear mode is 10228.8, and the wave number α at criticality is 1.274. Not surprisingly, the neutral stability curve for the superposed fluids is qualitatively similar in shape to that for a single fluid in plane Poiseuille flow. (Recall, from linear stability analysis of plane Poiseuille flow of a single fluid $R_c = 5772.2$ [2].) Note, the Reynolds number for the sample calculation is defined in terms of the properties of the upper layer, which is the less viscous of the two.

In Fig. 3 we have plotted the real and imaginary parts of the amplitude of the disturbance stream function (ϕ_1, ψ_1) for the shear mode at criticality ($R_c = 10228.8$, $\alpha = 1.274$). Near the wall $x = 1$, the imaginary part of the eigenfunction $\phi_1^{(i)}$ undergoes a rapid change in its derivative. Since the wave speed at criticality is $c_r = 0.8257$, and the critical point occurs at $x = 0.924$ (i.e., where $U_1(x) = c_r$), this suggests that the characteristic wiggle in $\phi_1^{(i)}$ is indicative of eigenfunction behavior in a critical layer. (The wiggle is not a consequence of round-off error from the numerical integration.)

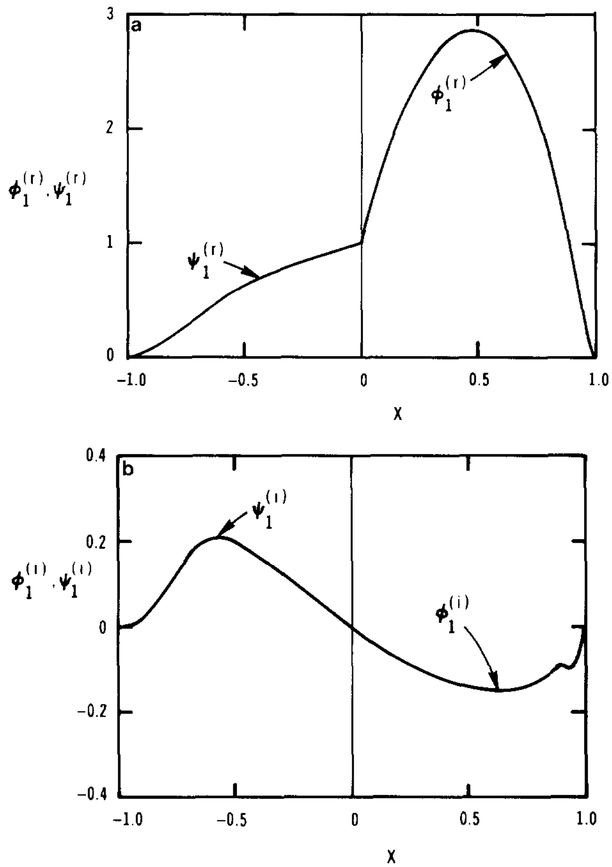

FIG. 3. (a) Real part of ϕ_1, ψ_1 for the shear mode at criticality. Flow parameters same as in Fig. 2. (b) Imaginary part of ϕ_1, ψ_1 for the shear mode at criticality. Flow parameters same as in Fig. 2.

To pursue this issue further, it is instructive to examine how the eigenfunction $\phi_1^{(i)}$ near a critical point evolves as the viscosity ratio is changed. For the purpose of comparison we consider the single fluid case $m = 1$, $R = 10{,}000$, $\alpha = 1$. The critical points for this flow occur at $x = \pm 0.8732$, and the eigenfunction $\phi_1^{(i)}$ exhibits characteristic extrema in the neighborhood of the critical points [2]. As m increases, the lower fluid spanning the region $-1 \leqslant x \leqslant 0$ becomes increasingly more viscous, and in the limit $m \to \infty$, it becomes passive with regard to any shear mode that is excited in the upper fluid. Consequently, in this limit the eigenfunction corresponding to the unstable shear mode will have similar characteristics to the eigenfunction for the single fluid case except it now will be centered around $x = 0.5$. Indeed, this is borne out in Fig. 4 where we have plotted the imaginary part of the amplitude of the disturbance stream function $(\phi_1^{(i)}, \psi_1^{(i)})$ for different viscosity ratios. In order to make clear the similarities with the single fluid case, we have normalized

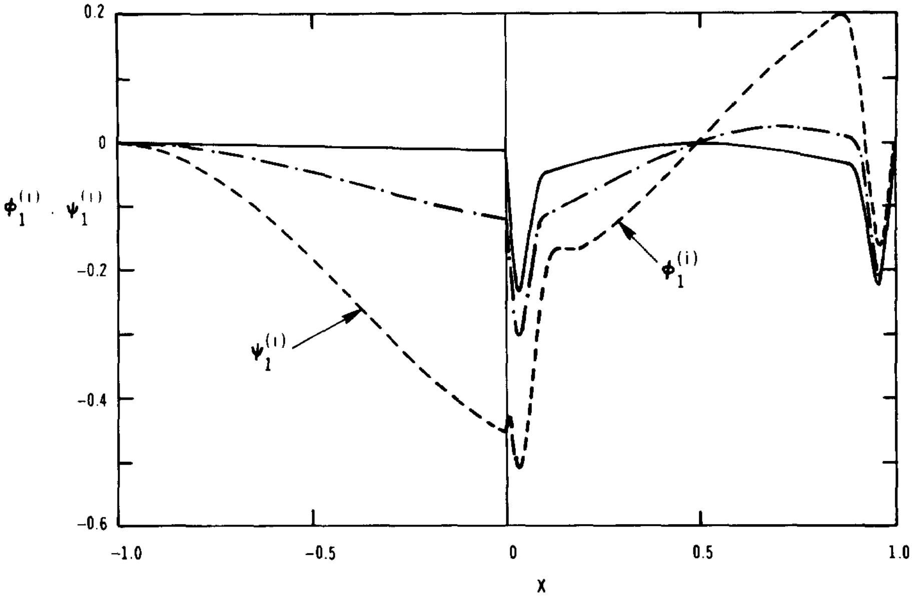

FIG. 4. Dependence of the imaginary part of ϕ_1, ψ_1 on viscosity ratio: — $R^* = 20{,}000$, $\alpha = 2$, $m = 10^6$; —·— $R^* = 20{,}000$, $\alpha = 2$, $m = 10^5$; - - - $R_c^* = 7534$, $\alpha = 2.16$, $m = 10^4$.

the eigenfunction ϕ_1 to be unity at $x = 0.5$ (instead of at $x = 0$) and have used the maximum velocity in the upper fluid as the characteristic velocity (instead of the interfacial velocity); the new definitions for the Reynolds number and wave speed are (for $n = 1$)

$$R^* = R[1 + (m-1)^2/8(m+1)]$$
$$c^* = c/[1 + (m-1)^2/8(m+1)].$$

In Table I we show how the locations of the critical points for the shear mode vary

TABLE I

Dependence of the Critical Points on Viscosity Ratio

Viscosity Ratio m	Reynolds number R^*	Wave number α	Wave speed c^*	Critical points	
				x_1	x_2
10^4 [a]	7,534	2.16	0.29177	0.07903	0.92076
10^5	20,000	2	$0.23780 + i0.00509$	0.06346	0.93651
10^6	20,000	2	$0.23755 + i0.00387$	0.06340	0.93659
∞ [b]	20,000	2	$0.23752 + i0.00373$	0.0634	0.9366

[a] Wave number and wave speed evaluated at criticality $R_c^* = 7{,}534$.
[b] Plane Poiseuille flow, Thomas [8].

with the viscosity ratio. For comparison, we also list the values for the wave speed and critical points for plane Poiseuille flow (Thomas [8]). Note, we have rescaled Thomas' values to account for the fact that the flow domain for $\phi_1^{(i)}$ is $0 \leqslant x \leqslant 1$, and not $-1 \leqslant x \leqslant 1$.

It is evident from Fig. 4 that for a viscosity ratio $m = 10^6$ ($R^* = 20{,}000$, $\alpha = 2$), $\phi_1^{(i)}$ is almost symmetric about $x = 0.5$ (as it should be when the lower fluid is passive), and is similar in shape to the eigenfunction computed by Thomas for plane Poiseuille flow (see also [2]). The wave speed and the critical points for this eigenfunction are in quantitative agreement with the values reported by Thomas (see Table I). When the viscosity ratio is decreased to 10^5, there is a marked change in $\phi_1^{(i)}$. The profile becomes noticeably skewed about $x = 0.5$, and $\psi_1^{(i)}$ increases in magnitude, indicating that the lower fluid can now no longer be regarded as

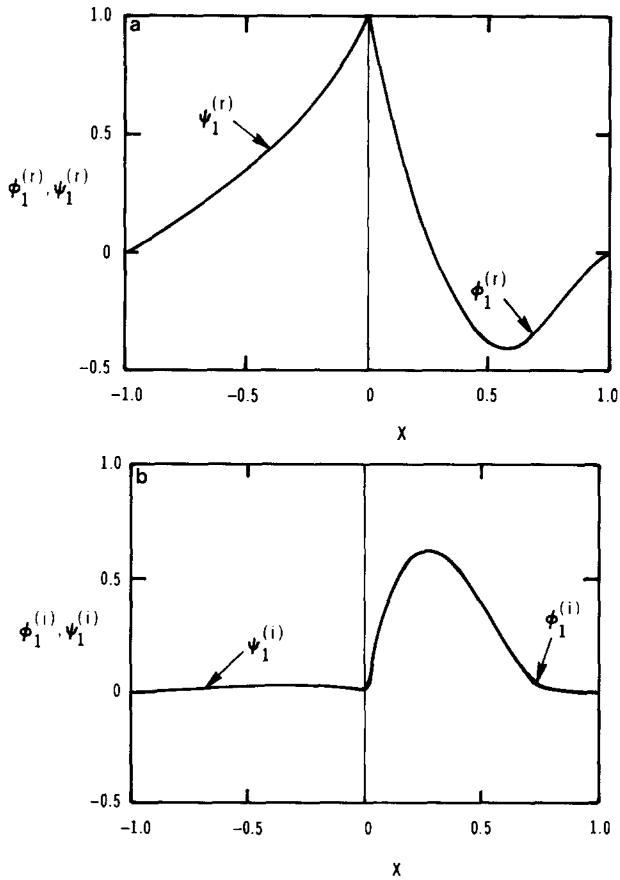

FIG. 5. (a) Real part of ϕ_1, ψ_1 for an unstable interfacial mode at $R = 10228.8$, $\alpha = 1.274$, and $c = 1.35653 + i0.23267$. Flow parameters same as in Fig. 2. (b) Imaginary part of ϕ_1, ψ_1 for an unstable interfacial mode at $R = 10228.8$, $\alpha = 1.274$, and $c = 1.35653 + i0.23267$. Flow parameters same as in Fig. 2.

passive. The influence of the lower fluid on $\phi_1^{(i)}$ is perhaps more evident for the case $m = 10^4$, $R_c^* = 7{,}534$, $\alpha = 2.16$ (Fig. 4, Table I). Note, these parameter values define a point on the neutral stability curve ($c_i = 0$). For this viscosity ratio there is a dramatic change in the shape and magnitude of $\phi_1^{(i)}$ near the interface $x = 0$. Our calculations show that there are no appreciable differences in the real part of the eigenfunctions ($\phi_1^{(r)}$, $\psi_1^{(r)}$) for the three cases shown in Fig. 4.

We now return to Fig. 2. Although the flow at $R = 10228.8$ is neutrally stable with respect to the shear mode, the flow is also unstable to an interfacial mode. In Fig. 5 we have plotted the eigenfunctions ϕ_1, ψ_1 corresponding to this unstable interfacial mode ($c_i > 0$). The wave speed for the interfacial mode at $\alpha = 1.274$, $R_c = 10228.8$ is $c = 1.35653 + i\,0.23267$. It is interesting to note that the growth rate for the interfacial mode, given by αc_i, need not be negligible. Indeed, as our calculations show, in many cases the growth rate for a shear mode is an order of magnitude or more smaller than that for the corresponding interfacial mode. Thus, the possibility exists for an interfacial mode to dominate flow instability even when an unstable shear mode is present. This issue and how it relates to the experiments of Kao and Park [3] is beyond the scope of this paper and is discussed elsewhere (Yiantsios and Higgins [9]).

4. Concluding Remarks

The advantages of the compound matrix method over other shooting techniques for solving difficult, eigenvalue and boundary value problems have been convincingly demonstrated by Ng and Reid [3–5] and Davey [1]. As we have shown in this paper, the method is capable also of solving eigenvalue problems with interfacial boundary conditions. Because an iterative technique is used to calculate the eigenvalues, a potential disadvantage of the compound matrix method is that one needs to have an initial guess for the eigenvalue and some knowledge of whether other modes are unstable. From our experience, we have found it useful to complement the compound matrix method with a method that calculates all the eigenvalues for the discretized problem (e.g., finite elements or finite difference), and then use the compound matrix method to refine the calculations for a particular mode. Thereafter, first-order continuation can be used with the compound matrix method to track a mode through a required parameter space.

Acknowledgment

This work was supported in part by the National Science Foundation Grant CBT-8505256, and by the University of California through a faculty research grant to Brian G. Higgins.

References

1. A. Davey, *J. Comput. Phys.* **35**, 36 (1980).
2. P. G. Drazin and W. H. Reid, *Hydrodynamic Stability* (Cambridge Univ. Press, Cambridge/New York, 1981), p. 221.
3. T. W. Kao and C. Park, *J. Fluid Mech.* **52**, 401 (1972).
4. B. S. Ng and W. H. Reid, *J. Comput. Phys.* **30**, 125 (1979).
5. B. S. Ng and W. H. Reid, *J. Comput. Phys.* **33**, 70 (1979).
6. B. S. Ng and W. H. Reid, *J. Comput. Phys.* **58**, 209 (1985).
7. B. Schwartz, *Pacific J. Math.* **32**, 203 (1970).
8. L. H. Thomas, *Phys. Rev.* (2) **91**, 780 (1953).
9. S. Yiantsios and B. G. Higgins, submitted for publication.
10. S. Yiantsios and B. G. Higgins, *Int. J. Num. Meth. Fluids* **7**, 247 (1987).
11. C. S. Yih, *J. Fluid Mech.* **27**, 337 (1967).